Unraveling the structure and function of CdcPDE: A novel phosphodiesterase from Crotalus durissus collilineatus snake venom

de Oliveira, Isadora Sousa; Pucca, Manuela Berto; Wiezel, Gisele Adriano; Cardoso, Iara Aimê; de Castro Figueiredo Bordon, Karla; Sartim, Marco Aurélio; Kalogeropoulos, Konstantinos; Ahmadi, Shirin; Baiwir, Dominique; Nonato, Maria Cristina

Total number of authors:
15

Published in:
International Journal of Biological Macromolecules

Link to article, DOI:
10.1016/j.ijbiomac.2021.02.120

Publication date:
2021

Document Version
Peer reviewed version

Unraveling the structure and function of CdcPDE: A novel phosphodiesterase from Crotalus durissus collilineatus snake venom

Isadora Sousa de Oliveira, Manuela Berto Pucca, Gisele Adriano Wiezel, Iara Aimê Cardoso, Karla de Castro Figueiredo Bordon, Marco Aurélio Sartim, Konstantinos Kalogeropoulos, Shirin Ahmadi, Dominique Baiwir, Maria Cristina Nonato, Suely Vilela Sampaio, Andreas Hougaard Laustsen, Ulrich auf dem Keller, Loïc Quinton, Eliane Candiani Arantes

PII: S0141-8130(21)00399-8

DOI: https://doi.org/10.1016/j.ijbiomac.2021.02.120

Reference: BIOMAC 17947

To appear in: *International Journal of Biological Macromolecules*

Received date: 11 December 2020

Revised date: 13 February 2021

Accepted date: 15 February 2021

Please cite this article as: I.S. de Oliveira, M.B. Pucca, G.A. Wiezel, et al., Unraveling the structure and function of CdcPDE: A novel phosphodiesterase from Crotalus durissus collilineatus snake venom, *International Journal of Biological Macromolecules* (2018), https://doi.org/10.1016/j.ijbiomac.2021.02.120

Unraveling the structure and function of *Cdc*PDE: A novel phosphodiesterase from *Crotalus durissus collilineatus* snake venom

Isadora Sousa de Oliveira[a], Manuela Berto Pucca[b], Gisele Adriano Wiezel[a], Iara Aimê Cardoso[a], Karla de Castro Figueiredo Bordon[a], Marco Aurélio Sartim[c,d], Konstantinos Kalogeropoulos[e], Shirin Ahmadi[e], Dominique Baiwir[f,g], Maria Cristina Nonato[a], Suely Vilela Sampaio[h], Andreas Hougaard Laustsen[e], Ulrich auf dem Keller[e], Loïc Quinton[f], Eliane Candiani Arantes[a,*]

[a]Department of BioMolecular Sciences, School of Pharmaceutical Sciences of Ribeirão Preto, University of São Paulo, Ribeirão Preto, SP, Brazil

[b]Medical School, Federal University of Roraima, Boa Vista, RR, Brazil

[c]Institute of Biological Sciences, Federal University of Amazonas, Manaus, AM, Brazil

[d]Department of Teaching and Research, Dr. Heitor Vieira Dourado Tropical Medicine Foundation, Manaus, AM, Brazil.

[e]Department of Biotechnology and Biomedicine, Technical University of Denmark, Kongens Lyngby, Denmark

[f]Mass Spectrometry Laboratory, Department of Chemistry, University of Liège, Liège, Belgium

[g]GIGA Proteomics Facility, University of Liège, Liège, Belgium

[h]Department of Clinical Analysis, Toxicology and Food Science, School of Pharmaceutical Sciences of Ribeirão Preto, University of São Paulo, Ribeirão Preto, SP, Brazil

***Corresponding author**

Dr. Eliane Candiani Arantes, Laboratory of Animal Toxins, Department of BioMolecular Sciences, School of Pharmaceutical Sciences of Ribeirão Preto, University of São Paulo. Av. do Café s/nº, Monte Alegre, 14040-903 – Ribeirão Preto, SP – Brazil, Phone: +55 (16) 33154275, Fax: +55 (16) 33154880, e-mail: ecabraga@fcfrp.usp.br.

Abstract

This study reports the isolation, structural, biochemical, and functional characterization of a novel phosphodiesterase from *Crotalus durissus collilineatus* venom (*Cdc*PDE). *Cdc*PDE was successfully isolated from whole venom using three chromatographic steps and represented 0.7% of total protein content. *Cdc*PDE was inhibited by EDTA and reducing agents, demonstrating that metal ions and disulfide bonds are necessary for its enzymatic activity. The highest enzymatic activity was observed at pH 8-8.5 and 37 °C. Kinetic parameters indicated a higher affinity for the substrate *bis*(*p*-nitrophenyl) phosphate compared to others snake venom PDEs. Its structural characterization was done by the determination of the protein primary sequence by Edman degradation and mass spectrometry, and completed by the building of molecular and docking-based models. Functional *in vitro* assays showed that *Cdc*PDE is capable of inhibiting platelet aggregation induced by adenosine diphosphate in a dose-dependent manner and demonstrated that *Cdc*PDE is cytotoxic to human keratinocytes. *Cdc*PDE was recognized by the crotalid antivenom produced by the Instituto Butantan. These findings demonstrate that the study of snake venom toxins can reveal new molecules that may be relevant in cases of snakebite envenoming, and that can be used as molecular tools to study pathophysiological processes due to their specific biological activities.

Keywords: *Crotalus durissus collilineatus*; phosphodiesterase; cytotoxicity.

1. Introduction

Snakebite envenoming is recognized as a Neglected Tropical Disease (NTD) by the World Health Organization (WHO) due to its high level of morbidity and mortality, as well as its frequency in impoverished regions of the tropics [1–5]. In Brazil, ~30,000 snakebite envenomings are reported each year, primarily caused by four genera, *Micrurus*, *Bothrops*, *Lachesis*, and *Crotalus* [6], being the last one represented by six subspecies, *C. durissus collilineatus*, *C. d. terrificus*, *C. d. marajoensis*, *C. d. ruruima*, *C. d. cascavella*, and *C. d. durissus* [7].

Crotalid venoms contain proteins with enzymatic and non-enzymatic activities [8,9]. Nucleases are among the enzymatic components that are able to hydrolyze nucleic acids and their derivates [10],

which can be subdivided into endonucleases [11] (DNAse [12] and RNAse [13]) and exonucleases, which include phosphodiesterases (PDE) [14]. PDEs are metalloglycoproteins [15–17] with high molecular mass (90 kDa ~ 160 kDa), found in the monomeric, homodimeric, or heterodimeric forms [17–22], which can hydrolyze phosphodiester bonds of polynucleotides in basic pH, starting at the 3'-extremity, resulting in 5'-mononucleotides [10]. In addition, PDEs can hydrolyze adenosine triphosphate (ATP) and adenosine diphosphate (ADP) to produce adenosine [10,18], nicotinamide adenine (NAD), and nicotinamide guanine dinucleotide (NGD) [10], as well as second messengers, such as 3',5'-cyclic adenosine monophosphate (cAMP), and 3',5'-cyclic guanosine monophosphate (cGMP) [23]. Due to their functionality, PDEs can play an important role in many physiological processes, including muscle contraction, cell differentiation, ion channel function, lipogenesis, gluconeogenesis, glycogenolysis, and apoptosis [24–26], may be considered as potential therapeutic candidates for treating different diseases such as cardiovascular, inflammatory, and Alzheimer's diseases, as well as erectile dysfunction [25–30].

PDEs are classified into eleven types (PDE1-11) according to their inhibitor-sensitivity, protein sequence, pharmacological properties and substrate specificity. PDE4, 7, and 8 are specific for cAMP degradation, whereas PDE5, 6, and 9 are specific for cGMP degradation, and PDE1, 2, 3, 10, and 11 for degrade both cAMP and cGMP [31,32].

Proteomic and transcriptomic data indicate that PDEs are found in several snake venoms [33–37], but in low abundance [38], and despite the wide distribution across different snake families, the role of these enzymes in snakebite envenoming has not been adequately explored [10]. Russell, Buess, and Woo (1963) partially purified the PDEs present in *C. adamanteus*, *C. atrox*, *C. viridis helleri*, *C. horridus*, and *Vipera russelli* venoms, reporting that PDEs were able to lead to hypotensive crisis in animals, characterized by low blood pressure and locomotor depression due to cAMP depletion [39]. This hypotensive effect of snake PDEs indicates that PDE substrates are available in the circulatory system of snakebite victims [10,40].

Since the discovery of PDEs in snake venoms (1932) [14], they have been used in nucleic acid characterization and as molecular biology tools [19]. They can act as platelet aggregation inhibitors [26,41,42] and may, eventually, become potential drug leads to treat dysfunctions related to increased platelet aggregation (e.g. thrombosis) [42].

Among nucleases, PDEs are relatively well-characterized; however, compared to other snake venom components, such as phospholipases, and serine and metalloproteases, studies focusing on PDEs are relatively rare. Here, we report the isolation, and structural and functional characterization of a novel PDE from *C. d. collilineatus* venom (*Cdc*PDE), and showcase its ability to inhibit platelet aggregation and induce cytotoxicity on human keratinocytes.

2. Methods

2.1. Venom fractionation and *Cdc*PDE purification

C. d. collilineatus snake specimen was collected from Catalão – GO (Brazil, 18º 10’ 12” S 47º 56’ 31” W) and kept in the Serpentarium of the University of São Paulo at Ribeirão Preto Medical School. Its venom was milked by compression of venom glands, dried in a glass vacuum desiccator for 6 hours at room temperature (RT) and stored at -20 °C until usage. This Serpentarium is accredited by the *Instituto Brasileiro do Meio Ambiente e dos Recursos Naturais Renováveis* (Brazilian Institute of Environment and Renewable Natural Resources), under the registration number 1506748.

Dried venom (90 mg) was resuspended in 50 mM Tris-HCl with 150 mM NaCl, pH 8, and centrifuged for 10 min at 13,000 × *g*, 4 ºC. The supernatant was fractionated on a HiPrep Sephacryl S-200 High-Resolution column (16 × 600 mm, 47 µm, GE Healthcare, Uppsala, Sweden). Fractions were eluted through an isocratic gradient with the same buffer at 0.5 mL/min flow rate. The fraction that showed the highest PDE activity (S3, 6 mg) was further fractionated through anion exchange chromatography in a HiTrap ANX (high sub) Sepharose Fast Flow column (16 × 25mm, GE Healthcare, Uppsala, Sweden), previously equilibrated with 50 mM Tris-HCl, pH 8. Elution was

performed using a linear gradient (0-1 M) of NaCl in the same buffer at a flow rate of 5 mL/min. The fraction that showed the highest PDE activity (A1, 0.7 mg) was fractionated through cation exchange chromatography in a 10 × 100 mm column packed with Carboxymethyl cellulose-52 (CMC-52, GE Healthcare, Uppsala, Sweden). Elution was performed using a segmented gradient from 0 to 100% of buffer B (50 mM sodium acetate (CH_3COONa) and 1 M NaCl, pH 5), at 0.5 mL/min flow rate. The column was previously equilibrated with buffer A (50 mM CH_3COONa, pH 5). In order to evaluate *Cdc*PDE purity and prepare the sample for structural assays, reversed-phase chromatography was performed with the fraction that showed the highest PDE activity (C2, 1 mg) in the cation exchange chromatography. For this purpose, a reversed-phase C4 Jupiter column (4.6 × 250mm, 5 µm, 300 Å, Phenomenex, Torrance, CA, USA), previously equilibrated with 0.1% trifluoroacetic acid (TFA), was used. The elution was performed using a linear gradient of 0-100% solution B (80% acetonitrile (MeCN) in 0.1% TFA) at a 1 mL/min flow rate. The eluted fraction was collected, frozen, and lyophilized for further analysis. All purification steps were performed at Fast Protein Liquid Chromatography Äkta Purifier UPC10 (GE Healthcare, Uppsala, Sweden) and automatically monitored at 280 nm. After each chromatographic step, the fractions of interest were concentrated using Amicon® Ultra-15 50K tube (Merck, São Paulo, SP, Brazil) at 4,000 × *g*, 4 ºC, for approximately 10 min. The protein amount was estimated by determining the sample's absorbance at 280 nm in a NanoDrop 2000 (Thermo Fisher Scientific Inc., Waltham, MA, USA).

2.2. *Cdc*PDE activity

*Cdc*PDE activity was determined according to Björk (1963) [43], with modifications proposed by Valério and colleagues (2002) [21], using a 96-well microplate and *bis*(*p*-nitrophenyl) phosphate (1 mM) as the substrate. Absorbance reading was performed in a microplate reader (Sunrise-basic, Tecan, Männedorf, Switzerland) at 400 nm. Enzyme activity was expressed as the percentage of activity

relative to the highest absorbance. According to Valério and colleagues (2002) [21], an increase of 1.0 $Abs_{400\ nm}$/min corresponds to 1 unit of enzymatic activity.

Catalytic activity of *Cdc*PDE (0.75 µg) was evaluated considering three variables: storage temperatures (-80, -20, 0, 4, 25, 37, 50, and 70 ºC; one hour), pH values (7, 7.5, 8, 8.5, 9, and 9.5), and reaction temperatures (0, 4, 25, 37, and 50 ºC). As positive control, PDE was previously incubated with 100 mM Tris-HCl, pH 8. Heat inactivated PDE (incubated for 10 min at 100 ºC) was used as negative control.

An enzymatic kinetic assay was carried out using different substrate concentrations (0-5 mM) in order to determine the parameters of the steady-state kinetics for *Cdc*PDE. Substrate hydrolysis was spectrophotometrically monitored at 400 nm, 25 °C, using the microplate reader SpectraMax Plus 384 (Molecular Devices, San Jose, CA, USA). All readouts were made in triplicates, at 3-second intervals for 20 min. The concentration of the product formed was estimated considering its extinction coefficient at 400 nm (17.6 $M^{-1}.cm^{-1}$) [17]. The kinetic constants (K_m and k_{cat}) were estimated using the equation for Michaelis-Menten kinetics:

$$V_0 = \frac{[E]\times k_{cat}\times [S]}{K_m + [S]}$$

V_0: Initial enzyme velocity;
[E]: Enzyme concentration;
[S]: Substrate concentration;
k_{cat}: Number of times that each enzyme site converts substrate to product per time (turnover number);
K_m: Michaelis-Menten constant.

For the enzyme inhibition assay, *Cdc*PDE was incubated for 30 min at 37 ºC with different concentrations (0.625-10 mM) of the following enzyme inhibitors: β-mercaptoethanol, cysteine, dithiothreitol (DTT), and ethylenediaminetetraacetic acid (EDTA). All enzymatic assays were performed in triplicates.

All data were processed and analyzed using the GraphPad Prism 8 software (GraphPad Software Inc., La Jolla, CA, USA).

2.3. SDS-PAGE and glycosylation

C. d. collilineatus whole venom (10 µg) and venom fractions containing *Cdc*PDE (5 µg) were subjected to 10% SDS-PAGE according to the Laemmli method (1970) [44], under reducing and non-reducing conditions. Low molecular mass (97.0-14.4 kDa, 17-0446-01, GE Healthcare, Uppsala, Sweden) and wide molecular mass (120-10 kDa, M00516s, GenScript, New Jersey, USA) markers were used. The gel was stained with *Coomassie® Brilliant Blue G-250* (Sigma-Aldrich, St. Louis, MO, USA).

In order to qualitatively evaluate the glycosylation, *Cdc*PDE (30 µg, 12 µL) was denatured and reduced with 5% SDS (1 µL) and 1 M DTT (1 µL), respectively, for 10 min at 95 ºC. After that, 10% Triton X-100 (2 µL) and 20 U of PNGase F (V4831, Promega, Madison, WI, USA) were added, and the mixture was incubated for three hours at 37 ºC. The reaction was stopped by heating the sample for 10 min at 100 ºC. The sample was analyzed by 10% SDS-PAGE and the gel was stained as mentioned above. Reduced *Cdc*PDE without PNGase F was used as a control.

2.4. Determining molecular mass and amino acid sequence

The average molecular mass of *Cdc*PDE (10 µg) was determined by matrix-assisted laser desorption/ionization with a time-of-flight analyzer (MALDI-TOF, RapifleX, Bruker Corporation, Billerica, MA, USA) using FlexControl 4.0 software (Bruker Corporation, Billerica, MA, USA) for data acquisition. The following parameters were employed in order to obtain data: 10,000 laser shots per spectrum and 500 Hz laser frequency. The instrument operated in linear positive mode, within a range of 20-220 kDa, and RapifleX was calibrated with bovine serum albumin (BSA, ~66 kDa $[M+H]^+$, ~33 kDa $[M+2H]^{2+}$, and BSA dimeric form ~132 kDa $[2M+H]^+$). As matrix, a saturated solution of sinapinic acid (SA) was prepared in MeCN and 0.1% TFA, at the ratio of 3:7. Data analysis was performed using the FlexAnalysis 3.4 software (Bruker Corporation, Billerica, MA, USA).

N-terminal sequencing was performed according to Edman's degradation method (1967) [45], using an automatic protein sequenator (PPSQ-33A, Shimadzu, Kyoto, Japan), following the

manufacturer's instructions. The obtained sequence was compared to databases through the Basic Local Alignment Search Tool (BLAST, https://blast.ncbi.nlm.nih.gov/Blast.cgi) [46], searching for similarity. For bottom-up approach, *Cdc*PDE (10 µg in 12 µL of 100 mM NH_4HCO_3) was reduced with 10 mM DTT (2 µL of 70 mM DTT) at 56 ºC, 600 rpm, for 40 min, and alkylated with 20 mM iodoacetamide (3 µL of 113.3 mM iodoacetamide) at RT for 30 min, in a dark compartment. Afterward, a second reduction with 11 mM DTT (2 µL of 104.5 mM DTT, RT, 5 min, dark compartment) was performed. This sample was digested with trypsin (2 µL of 0.1 µg/µL; ref. 90058, Thermo Fisher Scientific Inc., Waltham, MA, USA) with a ratio of 1:50 (trypsin:*Cdc*PDE), at 37 ºC, 600 rpm, overnight. After that, a second digestion with trypsin was performed with a ratio of 1:100 (trypsin:*Cdc*PDE) and acetonitrile 80% (92 µL of 100% MeCN) was added. The sample was kept at 37 ºC, 600 rpm, for 3 h. The reaction was stopped by adding 10% v/v TFA (6 µL), and the sample was desalted using a reversed-phase ZipTip® C18 column (ref. 87782, Thermo Fisher Scientific Inc., Waltham, MA, USA). Peptide mass fingerprint (PMF) of the protein was obtained using the same MALDI-TOF equipment mentioned above. RapifleX was however operated in reflectron positive mode and calibrated with a mixture of peptides (Peptide calibration standard, ~1000-3200 Da, ref. 206195, Bruker Corporation, Billerica, MA, USA). As matrix, a 10 mg/mL solution of 2,5-dihydroxybenzoic acid (DHB) was prepared in MeCN and 0.1% TFA, at a ratio of 1:1. Data analysis was performed through FlexAnalysis 3.4 and BioTools 3.2 (Bruker Corporation, Billerica, MA, USA). Digested peptides were submitted to MS/MS fragmentation through RapifleX, controlled by the software FlexControl 4.0 for data acquisition. MS/MS spectra were interpreted with FlexAnalysis 3.4 and Sequence Editor 3.2 (Bruker Corporation, Billerica, MA, USA).

For LC-MS/MS, three samples of *Cdc*PDE (10 µg each) were reduced and alkylated as described above. The first one (sample 1) was digested with trypsin, as described above. However, the other two samples (samples 2 and 3) were digested with a mixture of proteases containing trypsin (ref. 90058, Thermo Fisher Scientific Inc., Waltham, MA, USA), chymotrypsin (ref. 90056, Thermo Fisher

Scientific Inc., Waltham, MA, USA), and endoproteinase Glu-C (ref. 90054, Thermo Fisher Scientific Inc., Waltham, MA, USA) at different ratios (1 U trypsin : 85 µg *Cdc*PDE, 1 U chymotrypsin : 55 µg *Cdc*PDE, and 1 U endoproteinase Glu-C : 85 µg *Cdc*PDE), at 37 ºC, 600 rpm, for 2 h [47]. The reaction of samples 1 and 2 was stopped with 0.5% TFA. For sample 3, the reaction was stopped by an increase in temperature (to ~100 ºC), for 3 min, and this sample was digested with N-glycosidase F (ref 11365177001, lot 16070923, Roche, Basel, Switzerland), at the ratio of 5 U N-glycosidase F:100 µg of *Cdc*PDE, 37 ºC, 600 rpm for 4 h. After these steps, a second digestion with N-glycosidase F was performed, but with a different glycosidase-to-protein ratio and time (3 U N-glycosidase F:100 µg of *Cdc*PDE, overnight) at 37 ºC, 600 rpm. The reaction was stopped with 0.5% TFA. Digested materials were analyzed by Acquity UPLC® M-Class (Waters, Milford, MA, USA) coupled to a Q-Exactive™ Plus Hybrid Quadrupole-Orbitrap™ Mass Spectrometer (Thermo Fisher Scientific Inc., Waltham, MA, USA). High-resolution (70,000 at m/z 200) MS spectra from trypsin digestion were acquired within the scan range of 400-1750 m/z and with automatic gain control (AGC) target at $3e^6$. Subsequently, the twelve most intense ions (+2 or higher charge) were fragmented by higher-energy collisional dissociation (HCD, normalized collision energy of 25), in a data-dependent mode, in which high-resolution MS/MS spectra (17,500 at m/z 200) were acquired within the scan range of 200-2000 m/z and isolation window of ± 2 m/z, and with AGC target at $1e^5$. For those samples with multiple digestions, MS spectra were acquired with AGC target at $1e^6$ within the scan range of 400-1600 m/z, whereas MS/MS spectra were acquired with a normalized collision energy of 28. Other parameters remained the same. All MS/MS spectra were interpreted by automated *de novo* sequencing, using Peaks Studio 7 software (Bioinformatics Solutions Inc., Waterloo, Canada), against databases extracted by our group, generated from UniProt Knowledgebase (UniProtKB, https://uniprot.org)[48], which comprised protein sequences found in snake venoms (9,421 sequences, keyword "snake"), and PDE sequences from *Crotalus* venoms (17 sequences, keywords "phosphodiesterase" and "*Crotalus*") without signal peptide, both downloaded in June 2019. Parent mass and fragment mass error tolerance

were set to 5 ppm and 0.015 Da. Carbamidomethyl cysteine was set as a fixed modification, whereas amidation and methionine oxidation were considered as variable modifications. A maximum of 3 missed cleavages were allowed per peptide.

2.5. *Cdc*PDE sequence analysis, homology model, and docking simulation

The primary sequence of *Cdc*PDE was analyzed for the presence of domains using the conserved domains search tool [49], available at http://www.ncbi.nlm.nih.gov/Structure/cdd/wrpsb.cgi.

A three-dimensional model of *Cdc*PDE was constructed using the Swiss-Model web server (https://swissmodel.expasy.org/) [50], on automated mode [51]. Homology modeling was performed using the PDE from Taiwan cobra (*Naja atra*) as a template (PDB ID: 5GZ4), which was the top hit in the template search (GMQE: 0.94, Sequence identity: 85.01%).

Docking simulation was performed with SwissDock [52,53], using default parameters. SwissDock is based on an algorithm that generates multiple binding modes, estimating their CHARMM force field energies in a grid, evaluating binding energies, and selecting the most favorable ones. The ligand structure was identified in the PubChem database (PubChem CID: 255), and the structure data file (SDF) was used along with the aforementioned *Cdc*PDE model in the molecular docking simulations. The model built of *Cdc*PDE was validated using the PROCHECK (https://servicesn.mbi.ucla.edu/PROCHECK/) [54,55] and ERRAT (https://servicesn.mbi.ucla.edu/ERRAT/) [56] webservers. The final output docked models were visualized and analyzed with the CHIMERA software package (https://cgl.ucsf.edu/chimera/) [57].

2.6. *Cdc*PDE thermal stability

Differential scanning fluorimetry (Thermofluor) was used to evaluate *Cdc*PDE thermal stability. The experiment was carried out in a thermocycler Mx3005P (Agilent Technologies, Santa Clara, CA, USA), using SYPRO® orange (492/610 nm) as a fluorescent probe in a 96-well PCR plate. The behavior of *Cdc*PDE at different pH and ionic strengths was assayed using Solubility & Stability Screen 2 (Hampton Research). The 20 µL reaction mixture contained 1 mg/mL of *Cdc*PDE and 50× SYPRO®

orange. The samples were heated from 25 to 95 °C, at 1 °C/min increase rate, and fluorescence was measured every minute. Thermal melting curves were processed according to the protocol described by Niesen and colleagues (2007) [58], and the melting temperature was calculated using GraphPad Prism 8 software.

2.7. Recognition of crotalid antivenom against *Cdc*PDE and prediction of molecule epitopes

An ELISA assay was performed using a 96-well microplate (Costar, Corning Incorporated, NY, USA) coated with *Cdc*PDE (2 µg) and *C. d. collilineatus* whole venom (2 µg) in 0.05 M carbonate/bicarbonate buffer, pH 9.6 (100 µL/well). As positive control, some wells were coated with non-immunized horse serum (1:50, H0146, lot SLBS7574, Sigma-Aldrich, St. Louis, MO, USA) in 0.05 M carbonate/bicarbonate buffer, pH 9.6. The plate was incubated for 16 h at 4 ºC, then was washed three times with phosphate-buffered saline (PBS), pH 7.2. Afterward, the plate was blocked by adding 250 µL of PBS containing 2% (w/V) non-fat dry milk (Molico, Nestlé, Bebey, Switzerland; MPBS) and incubated for 2 h at 37 ºC. The plate was then washed three times with PBS-0.05% Tween (PBS-T) and three times with PBS and incubated for 1 h at 37 ºC with anti-crotalid antivenom (1:100 in 1% MPBS). As negative control, *Cdc*PDE and venom coated wells were incubated with non-immunized horse serum diluted 1:100 in 1% MPBS. The plate was washed three times with PBS-T and PBS, respectively. After that, the plate was incubated with 100 µL of anti-horse polyclonal antibodies conjugated with peroxidase (IgG-HRP, A6915, Sigma-Aldrich, St. Louis, MO, USA) diluted 1:3000 in 1% MPBS. After one hour of incubation at 37 ºC, the plate was washed three times with PBS-T and three times with PBS. To each well, 100 µL of *o*-phenylenediamine dihydrochloride (OPD)-H_2O_2 (SIGMAFAST OPD tablet, SLBM4528V, Sigma-Aldrich, St. Louis, MO, USA), diluted according to the manufacturer's instructions, were added. Finally, the plate was incubated in a dark chamber at RT until color development. Then, the reaction was stopped with 50 µL of 1 M H_2SO_4 (Merck, São Paulo, SP, Brazil). Absorbance was measure at 490 nm on a 96-well plate reader (Sunrise-basic Tecan, Männedorf,

Switzerland). The assay was carried out in quadruplicates, and the results were analyzed by one-way ANOVA, followed by Tukey's post-hoc test ($p < 0.05$).

ABCpred Server, with a threshold of 0.9 and a window length of 14 to 16 residues, was used to predict which *Cdc*PDE epitopes are recognized by B cells (http://crdd.osdd.net/raghava/abcpred/) [59].

2.8. Platelet aggregation assay

Human peripheral blood samples (~10 mL) were collected with a conventional citrate collection tube (Vacutainer, BD Biosciences, Franklin Lakes, Nova Jersey, USA) from 10 voluntary donors (both genders; 20 to 40 years old; without medical history of taking oral anticoagulants that could interfere with the blood clotting process) and centrifuged at 1,000 rpm (112 rcf), RT, for 10 min, to obtain platelet-rich plasma (PRP). PRP (450 µL) was incubated for 5 min under constant agitation. Different concentrations of *Cdc*PDE (15-120 µg/mL) and/or ADP (2,4 µM) were added and platelet aggregation was monitored for 6 min using an optical aggregometer (Chrono-Log Corporation, Havertown, PA, USA). The assay was performed in triplicates, and results were analyzed by one-way ANOVA followed by Dunnett's post-hoc test ($p < 0.05$).

This assay was performed after approval of the research project by *Comitê de Ética em Pesquisa* (Research Ethics Committee), School of Pharmaceutical Sciences of Ribeirão Preto (FCFRP-USP), under the protocol no. 435 – CAAE no. 64850717.8.0000.5403.

2.9. Cytotoxicity assay in human keratinocytes (N/TERT cells)

Immortalized human keratinocyte cells (N/TERT, 4×10^3) were seeded in a 96-well polystyrene black opaque plate (ref. 237105, Thermo Fisher Scientific, Roskilde, Denmark) and cultured in Dulbecco's modified Eagle's medium (DMEM: F12; Grand Island, NY, USA) with 1% penicillin-streptomycin and supplemented with 10% fetal bovine serum (FBS) and 1× RM plus supplement. The plate was incubated at 37°C, with 5% CO_2 and 85% humidity overnight. After this period, the medium was aspirated, and fresh medium containing different concentrations of *Cdc*PDE (10-200 µg/mL) was

added. The plate was incubated for 24 h at the same conditions mentioned before. Cell viability was determined with CellTiter-Glo luminescent cell viability assay (Promega, Madison, WI, USA), according to the manufacturer's instructions. The IC_{50} value was calculated with log(*Cdc*PDE) *versus* normalized response and Hill equation, using the GraphPad Prism 8 software (GraphPad Software Inc., La Jolla, CA, USA).

3. Results

*Cdc*PDE was successfully isolated from *C. d. collilineatus* venom through the three following chromatographic steps: size exclusion, anion, and cation exchange. The evaluation of *Cdc*PDE activity, using the specific substrate for PDEs (*bis*(*p*-nitrophenyl) phosphate) was performed on each fraction of all chromatographic steps to look for the presence of active *Cdc*PDE and select the fraction that would be used in the next steps (Fig. 1A-C). The third chromatographic step (cation exchange) was efficient in the final purification of the enzyme, but it must have induced some conformational change in the enzyme that caused a reduction in its specific activity. Therefore, the fraction A1 (non-pure *Cdc*PDE obtained after the second chromatographic step showing the highest specific activity) may be more suitable than C2 (pure *Cdc*PDE obtained after the third chromatographic step) for applications where the catalytic function is more relevant than the purity of the enzyme. Since fraction C2 corresponds to the pure and active *Cdc*PDE (Fig. 2A-B), this fraction was used in the enzymatic and functional assays. Although PDE activity was not detected after reversed-phase chromatography, this additional step was used to guarantee the *Cdc*PDE purity (Figure 1D shows the degree of purity for *Cdc*PDE after the third chromatographic step). This pure fraction (R) was only used in the assays in which the enzymatic activity was not relevant, such as mass spectrometry and other structural characterization assays (*e.g.* SDS-PAGE). It was also determined that the *Cdc*PDE enzyme corresponded to 0.71% of soluble proteins from *C. d. collilineatus* venom (Table 1).

After each step of *Cdc*PDE isolation, each fraction was analyzed by SDS-PAGE under reducing and non-reducing conditions. From the electrophoretic profiles, it was possible to infer that *Cdc*PDE

migrated as a monomer since it presented the expected mass for a classical PDE monomer (~90 kDa), both in reducing and non-reducing conditions. This assay confirms that the enzyme does not form covalently linked dimers; however, additional studies are needed to determine whether formation of non-covalently linked dimers may occur. In addition, it was possible to observe a difference of ~9 kDa between the reduced *Cdc*PDE and the reduced *Cdc*PDE digested by PNGase (Fig. 2C), evidencing the presence of N-glycosylations in *Cdc*PDE structure. The entire macromolecule had a mass $[M+H]^+$ of 100,330 and 105,598 Da determined by MALDI-TOF (Fig. 2D). These two masses could correspond to two different *Cdc*PDE isoforms or glycoforms.

*Cdc*PDE showed maximal activity between pH 8 and 8.5 on the substrate *bis*(*p*-nitrophenyl) phosphate (Fig. 3A). pH 8 was consequently chosen for the next experiments. *Cdc*PDE retained its best activity when stored at 0 °C (Fig. 3B) and the temperature that showed the highest activity was 37 °C (Fig. 3C). For the enzymatic kinetics assays, 15 different substrate concentrations were tested, and the product formation curves are shown in Fig. S1. *Cdc*PDE activity follows the Michaelis-Menten model, showing a hyperbolic kinetic curve when V_0 is plotted as a function of the substrate concentration (Fig. 3D). The K_m was 0.38 ± 0.03 mM, and k_{cat} was 0.14 ± 2.7×10^{-3} s^{-1}, while its catalytic efficiency (k_{cat}/K_m) was 0.37 ± 0.03 $mM.s^{-1}$. Another assay demonstrated that the lyophilization process led to a high loss of enzyme activity (data not shown); thus, *Cdc*PDE was not lyophilized prior to enzymatic assays. Regarding inhibitors, *Cdc*PDE activity decreased in a dose-dependent manner in all tested concentrations of β-mercaptoethanol (Fig. 3E), whereas for the other inhibitors (cysteine, DTT, and EDTA) *Cdc*PDE was completely inhibited at all tested concentrations (Table S1). Reference (water) melting temperature (T_m) for *Cdc*PDE was 65.71 ºC. Melting curves revealed a gain in thermal stability in almost all tested buffers, so that the greatest ΔT_m was obtained at pH 5.5 in the absence of salt. In comparison, the protein thermal stability was compromised at pH 4.5 (Fig. 4).

Following the characterization of *Cdc*PDE primary structure, the first 26 residues of the N-terminal region were sequenced through Edman degradation. In MS/MS analyzes, when the sample was digested only with trypsin (sample 1), 29,086 spectra generating 1,822 peptides were obtained. However, when the Multi-Enzymatic Limited Digestion (MELD) was performed (sample 2), 82,481 spectra and 8,889 peptides were generated. In addition, digesting the sample with MELD and N-glycosidase F (sample 3) generated 82,955 spectra and 13,062 peptides. All these results together generated a primary sequence of 829 amino acid residues. Finally, the PMF gave a sequence coverage of almost 72% of the proposed sequence. From these results, we identified 33 conserved cysteine residues and the three potential sites for N-glycosylation conserved in PDEs, except in J3SBP3 (which does not present the first putative N-glycosylation site). Interestingly, two additional sites for N-glycosylation were also identified. Moreover, the metal ion-binding/active site residues were fully conserved. *In silico* analysis of *Cdc*PDE primary structure revealed the presence of four domains: a somatomedin B domain (residues from 11 to 48), a somatomedin B-like domain (residues from 52 to 95), an ectonucleotide pyrophosphatase/phosphodiesterase domain – also called autotaxin – (residues from 117 to 483), and a DNA/RNA non-specific domain (residues from 581 to 810). Finally, the sequence obtained is similar to other snake venom PDEs, sharing more than 90% sequence identity. The determined sequence and its alignment with others PDEs are shown in Fig. 5, while the PMF and the spectra analyzed by *de novo* sequencing are shown in the supplementary material (Fig. S2, S3, and S4).

Additionally, with the obtained *Cdc*PDE primary sequence, it was possible to predict/model the secondary and tertiary structures. Molecular modeling suggests that *Cdc*PDE is composed of 22.7% α-helices, 16.4% □-strands, 4% 3_{10} helices, 20.2 % coils, and 35.2% turns, besides sixteen disulfide bonds (Fig. 6A-B). The structural model of *Cdc*PDE is complex, similar to the structures of other members of the alkaline phosphatase-like superfamily (ALP-like superfamily). The GMQE value obtained for this model was 0.94 and QMEAN was determined to -2.64. The PROCHECK analysis showed that >99% of the amino acid residues are in the most favored and allowed regions of the corresponding

Ramachandran plot, and the ERRAT analysis showed an overall quality factor of 87.22 for the *Cdc*PDE model.

Afterwards, docking simulation was used to predict the interaction of *Cdc*PDE and *bis*(*p*-nitrophenyl) phosphate substrate. The simulation demonstrated both the interactions of the residues (D125, T163, H167, D283, H287, D330, and H440) that seem to coordinate with the divalent metal cations (*e.g.* zinc) in the active site, and the close interaction of T163 residue with the substrate (Fig. 6C-E).

In a different assay, *Cdc*PDE was incubated with the commercial crotalid antivenom to assess the antivenom's ability to recognize this protein. The results showed that the Brazilian crotalid antivenom was able to efficiently recognize the enzyme (Fig. 7A). The result was not surprising since it was predicted *in silico* that there are 16 epitopes of the enzyme that could be recognized by B cells triggering an antibody response (Fig. 7B).

In functional assays, *Cdc*PDE inhibited ADP-induced platelet aggregation in a dose-dependent manner (Fig. 8A and S5). In addition, *Cdc*PDE showed cytotoxic activity against human keratinocytes in concentrations higher than 10 µg/mL (Fig. 8B), presenting an IC_{50} value of 71.65 µg/mL (Fig. S6).

4. Discussion

In Brazil, envenomings caused by *Crotalus* snakes represented almost 9% of the total snakebite cases in 2019 [6]. Although it is a low percentage, these accidents are responsible for severe envenomings, leading to high fatality rates [6,60]. Thus, studying the venoms from *Crotalus* snakes and their isolated components is of high importance to produce effective antivenoms against them. Since the elucidation of the proteomes and transcriptomes of many snake venoms, studies on nucleases have been prominent because of their presence in numerous snake families [19,38]. However, additional studies regarding their functions during envenoming are needed.

In our study, *Cdc*PDE isolation was achieved through three chromatographic steps. The first step, *i.e.* molecular filtration, was crucial for separating *Cdc*PDE from smaller components, such as

crotoxin, an enzyme complex constituting 65-68% of the crotalid venom [61]. In the two additional separation steps (anion exchange followed by cation exchange chromatography), the proteins were purified according to their charge. Basic pIs of PDEs have been previously reported to be between 7.4 and 10.5 [17,20,21,62]. Similarly, in this study, it was seen that at pH 8, *Cdc*PDE did not interact with the cationic resin used in the anion exchange chromatography. Therefore, *Cdc*PDE pI was predicted to be higher than 8. In the cation exchange chromatography step, which was performed at pH 5, *Cdc*PDE seemed to acquire a positive charge, allowing it to interact with the column, and, with the ionic strength increasing (NaCl concentration), *Cdc*PDE was eluted.

After completing the process of *Cdc*PDE isolation, we verified that *Cdc*PDE proportion in soluble venom is in accordance with the PDE yields (less than 1%) previously reported for *C. ruber ruber* [20], *Trimeresurus mucrosquamatus* [63], and *Daboia russelli russelli* venoms [42].

Our study indicated that *Cdc*PDE migrated as a monomeric protein, as previously described for PDEs from *Agistrodon bilineatus* [64] and *Bothrops alternatus* [21] venoms, named class 1 PDEs [64]. In addition, the N-deglycosylation assay followed by SDS-PAGE showed that *Cdc*PDE is a N-glycosylated protein, which increases its molecular mass by ~9% (considering the determined molecular mass of the primary structure, 94,154 Da). PDEs from *C. adamanteus* and *Vipera lebetina* venoms present nine potential N-glycosylation sites [22,65], whereas no carbohydrates were reported to be linked to the other snake venom PDEs [63,66]. This post-translational modification may be involved in the stability of the molecule. In addition, glycosylation may have an effect on inflammatory reactions and cellular signaling [67,68], as well as it may contribute to snake venom diversity through changing toxin conformation and, consequently, its function [69–72].

*Cdc*PDE molecular masses are quite similar to other monomeric PDEs, such as those reported from *Cerastes cerastes* (110 kDa) [66] and *B. alternatus* (105 kDa) venoms [21]. However, in these two cases, PDE molecular masses were estimated by SDS-PAGE while the methodology used in our study is more accurate. There are possibly two isoforms or glycoforms of *Cdc*PDE in the venom, since there

were two molecular masses determined; and it is known that snake venom may contain more than one PDE isoform [73]. Thus, it is possible that *Cdc*PDE molecules with different glycosylation patterns or partially cleaved by proteases are present in the venom.

Regarding *Cdc*PDE enzyme activity, it is known that exonucleases have greater activity at basic pH [10]. Our results corroborate with this finding. However, different PDEs may show maximal activity at different basic pH, *e.g.* PDEs from *B. alternatus* (pH ranging from 7.5 to 9.5) [21], *V. lebetina* (pH 8.8) [22], and *A. bilineatus* (pH ranging from 9 to 11) [64].

Previous studies show that the optimum temperature for PDEs varies between 55-60 °C, with loss of activity occurring at temperatures between 65-70 °C [20,21,43,62,63,66,74], but *Cdc*PDE showed its maximum activity at 37 °C. This difference could be correlated to the experimental conditions, such as pH and salinity of the buffer, used to measure the PDE activity. Also, in our experimental setup, the highest temperature evaluated was 50 °C, which presented ~72% of the PDE activity, indicating the initial decay of enzyme activity. Furthermore, the Thermofluor analysis suggests that the loss of enzyme activity reported for PDEs at temperatures above 65 °C may be related to the unfolding caused by an increase in temperature.

In addition, we observed that water loss during vacuum centrifugation or lyophilization can lead to more than 30% and 90% reduction in enzyme activity, respectively. This observation corroborates with the findings of Björk (1963) that evidenced a reduction of more than 25% in PDE activity after lyophilization [43].

Regarding kinetic parameters, although the *Cdc*PDE K_m (0.38 mM) is lower than those described for PDEs obtained from other snakes, such as *B. jararaca* (21.88 mM) [41], *B. alternatus* (2.69 mM) [21], and *C cerastes* (4.33 mM) [66], it is very close to the K_m value of *D. russelli* PDE (0.308 mM) [42]. The low K_m value of the *D.russelli* PDE and *Cdc*PDE show that these enzymes have 7 to 57 times more affinity for the used substrate compared to the aforementioned PDEs. On the other hand, *Cdc*PDE k_{cat} (0.14 s^{-1}) is higher than that observed for the *B. jararaca* PDE (4.4 x 10^{-4} s^{-1}) [41];

while catalytic efficiency was determined to 0.37 $mM.s^{-1}$ for *Cdc*PDE and 2×10^{-5} $mM.s^{-1}$ for the *B. jararaca* PDE, indicating a greater kinetic effectiveness of *Cdc*PDE. However, since the reaction buffer pH is not similar, the differences observed in the catalytic constants could be related to the different physico-chemical environment.

Inhibition of *Cdc*PDE by β-mercaptoethanol in a dose-dependent manner has also been observed in other PDEs, such as those from *B. alternatus* [21] and *C. cerastes* [66]. Total *Cdc*PDE inhibition caused by other reducing agents, such as DTT and cysteine, suggests that disulfide bonds may be essential for the enzymatic activity, as it has been described for the PDE from *N. nigricollis* venom [75]. In our study, *Cdc*PDE, similarly to many other PDEs [18,66,74], was inhibited by EDTA. Knowing that EDTA is a metal chelating agent, our result indicates that *Cdc*PDE is a metalloenzyme similar to many other PDEs, including PDE from *C. adamanteus* venom that presents zinc, magnesium, and calcium in its structure [15], PDE from *Trimeresurus stejnegeri* venom that presents zinc and copper in its structure [26], and PDE from *D. russelli* venom that presents only zinc in its structure [42].

*Cdc*PDE primary structure was determined through a combination of Edman degradation and mass spectrometry, using tryptic digestion and MELD. The use of MELD method is known to present some advantages, including the high number and diversity of the obtained peptides. In addition, MELD gives a higher percentage of protein coverage, facilitating the sequencing [47]. Combining the sequencing methods applied, it was observed that *Cdc*PDE shares a high sequence identity with other snake PDEs, as described above. It was also noted that *Cdc*PDE has two sites for N-glycosylation (NFS and NGS, at positions 194-196 and 237-239, respectively) alongside three more potential sites (NET, NLT, and NHS, at positions 17-19, 383-385 and 572-574 respectively). This suggest that the same PDE isoform with differences in their glycosylation pattern (*i.e.* either in quantity or in type of glycosylation) may be present in the venom. Our results corroborate with findings reported for PDEs from *V. lebetina*

and *C. adamanteus* venoms, in which 33 cysteines and 9 putative N-glycosylations sites were observed [22,65].

As mentioned earlier, PDEs can be present in snake venoms in different forms. In this study, based on the SDS-PAGE results and the template (5GZ4), we modeled the *Cdc*PDE in a monomeric form. A monomeric model of PDB previously built by Ullah and colleagues (2019) displays the same number of disulfide bonds as our *Cdc*PDE model (16 disulfide bonds) [65]. Moreover, both models show a divalent metal cation in the active site of the enzyme that is in accordance with other snake and human PDE findings [15,20,65,76]. Therefore, possessing the conserved metal ion-binding/active site residues and being inhibited by EDTA, *Cdc*PDE was determined to be a metalloenzyme. In addition, substrate binding was predicted to occur in the active site, directly interacting with T163, and the substrate positioning seems to agree with observation of how AMP is bound to the PDE from Taiwan cobra (*Naja atra*) (PDB ID: 5GZ5). Further support can be found from previous reports, where the T163 residue was demonstrated to be important for the enzymatic activity of other snake venom PDEs [22,65].

Currently, the only available treatment for snakebite envenoming is administration of animal plasma-derived antivenom [77,78], and it is possibly medically important that anti-crotalid antivenom recognizes *Cdc*PDE. Our results demonstrate that the tested Brazilian antivenom specifically recognizes both venom and PDE from *C. d. collilineatus*. Despite being present in small proportions in snake venoms [38], it is not surprising that crotalid antivenoms comprises specific antibodies targeting *Cdc*PDE, since it is a high molecular weight protein with likely high immunogenicity. Some authors suggest that the ideal size for epitopes that have immunogenicity is greater than 10 and not more than 20 residues [79,80]. Indeed, our epitope prediction revealed that the enzyme presents sixteen epitopes of such lengths that could possibly be recognized by the immune system.

The functional activities induced by the *Cdc*PDE were also explored in this study. Known as inhibitors of platelet aggregation, PDEs can hydrolyze ADP, an agonist that leads to aggregation [10].

Our results demonstrated that *Cdc*PDE reduces ADP-induced platelet aggregation as it was previously demonstrated for PDEs from venoms of *B. jararaca*, *D. russelli*, and *T. stejnegeri* [26,41,42]. Physiologically, injuries occurring in blood vessels lead to ADP-induced platelet aggregation, forming a blood clot. However, when this activation is not controlled, thrombus formation can occur, which causes further damage to the body [81,82]. Thus, *Cdc*PDE could be a promising molecule to study thrombosis. It may even find a potential therapeutic application similar to Tirofiban (Aggrastat®) and Eptifibatide (Integrilin®) that are snake-derived drugs capable of inhibiting platelet aggregation approved by the US Food and Drug Administration (FDA) [83,84].

This study also demonstrated that *Cdc*PDE has a cytotoxic effect on human keratinocytes. *Cdc*PDE decreased the viability of N/TERT cells with an LC_{50} of 71.65 µg/mL. Different cellular assays have been developed to evaluate the cytotoxicity of toxins *in vitro* [85–88], however, there are few studies using human keratinocytes to assess cytotoxicity of snake toxins [89,90], being our study pioneer to demonstrate that a PDE from snake venoms is cytotoxic to human keratinocytes. Since skin cells are usually affected in snakebite envenomings [91,92], it is relevant to evaluate the effect of snake toxins in keratinocytes. Although the local effects of crotalid envenoming are less evident than systemic effects [93], additional studies are needed to understand the local effects of crotalid toxins. Unfortunately, functional *Cdc*PDE studies could not be expanded due to the low yield of the enzyme.

5. Conclusion

Here, we report the isolation and characterization of a novel snake PDE from *C. d. collilineatus* venom, *i.e. Cdc*PDE. Only few studies on snake PDEs are available in the literature, and our study thus contributes to expanding the knowledge on this enzymatic toxin class by providing data on protein structure, enzymatic activity, thermostability, and cytotoxicity, as well as a structural protein-substrate interaction model. This study highlights cytotoxicity properties of *Cdc*PDE on human keratinocytes, which could be further explored to strengthen our knowledge on local effects of rattlesnake envenomings. Finally, PDEs could become important research or therapeutic tools, since they present

several biochemical functions that could be exploited to manipulate physiological and pathological processes, such as platelet aggregation.

Funding

This study was supported by *Fundação de Amparo à Pesquisa do Estado de São Paulo* (FAPESP, São Paulo Research Foundation, scholarships to ISO 2017/03580-9 and 2018/21233-7, GAW 2017/00586-6 and grants 2011/23236-4 and 2019/10173-6), *Coordenação de Aperfeiçoamento de Pessoal de Nível Superior* (CAPES, Coordination for the Improvement of Higher Education Personnel, Finance Code 001), *Conselho Nacional de Desenvolvimento Científico e Tecnológico* (CNPq, The National Council for Scientific and Technological Development, scholarship to MBP 307155/2017-0 and grant 306479/2017-6), and the Villum Foundation (grant 00025302). UK acknowledges support by a Novo Nordisk Foundation Young Investigator Award (NNF16OC0020670). Mass spectrometers used for this project were supported by the Walloon Region (Belgium) and the European Regional Development Fund (ERDF).

CRediT author statement

ISO was responsible for project development, designed the experimental approaches, interpreted the data, and wrote the manuscript. GAW, IAC, KCFB, KK, SA, and MCN contributed in purification and characterization assays. MBP, MAS, SVS, AHL, and UK contributed with the functional assays. DB and LQ contributed with mass spectrometry analysis. ECA coordinated and designed all the experiments, analyzed and interpreted the data. All authors read, corrected, and approved the final manuscript.

Competing interests

The authors declare that they have no competing interests.

References

[1] J.J. Calvete, Y. Rodríguez, S. Quesada-Bernat, D. Pla, Toxin-resolved antivenomics-guided assessment of the immunorecognition landscape of antivenoms, Toxicon. 148 (2018) 107–122.

https://doi.org/10.1016/j.toxicon.2018.04.015.

[2] J.M. Gutiérrez, J.A. Pereañez, The need for an integrated approach in confronting snakebite envenoming in latin america: the relevance of endogenous scientific and technoogical research, Vitae. 23 (2016) 103–105. https://doi.org/10.17533/udea.vitae.v23n2a01.

[3] L.S. Cruz, R. Vargas, A.A. Lopes, Snakebite envenomation and death in the developing world, Ethn Dis. 19 (2009) S1-42–6.

[4] World Health Organization, ed., Rabies and envenomings: a neglected public health issue ; report of a consultative meeting, World Health Organization, Geneva, 19 January 2007, WHO, Geneva, 2007.

[5] F.M.O. Pinho, I.D. Pereira, Ofidismo, Rev. Assoc. Med. Bras. 47 (2001) 24–29. https://doi.org/10.1590/S0104-42302001000100026.

[6] Ministério da Saúde, Acidentes por animais peçonhentos - Notificações registradas no Sistema de Informação de Agravos de Notificação - Brasil, (2020). http://tabnet.datasus.gov.br/cgi/deftohtm.exe?sinannet/cnv/animaisbr.def (accessed August 16, 2020).

[7] H.C. Costa, R.S. Bérnils, Répteis do Brasil e suas Unidades Federativas: Lista de espécies, Herpetologia Brasileira. 7 (2018).

[8] J.J. Calvete, Venomics: integrative venom proteomics and beyond, Biochem. J. 474 (2017) 611–634. https://doi.org/10.1042/BCJ20160577.

[9] J.J. Calvete, P. Juárez, L. Sanz, Snake venomics. Strategy and applications, J Mass Spectrom. 42 (2007) 1405–1414. https://doi.org/10.1002/jms.1242.

[10] B.L. Dhananjaya, C.J.M. D Souza, An overview on nucleases (DNase, RNase, and phosphodiesterase) in snake venoms, Biochemistry Mosc. 75 (2010) 1–6. https://doi.org/10.1134/s0006297910010013.

[11] C. Delezenne, H. Morel, Action catalytique des venins des serpents sur les acids nucleiques, CR Acad. Sci. (1919) 244–246.

[12] A.R. Taborda, L.C. Taborda, J.N. Williams, C.A. Elvehjem, A study of the desoxyribonuclease activity of snake venoms, J. Biol. Chem. 195 (1952) 207–213.

[13] A.R. Taborda, L.C. Taborda, J.N. Williams, C.A. Elvehjem, A study of the ribonuclease activity of snake venoms, J. Biol. Chem. 194 (1952) 227–233.

[14] S. Uzawa, Über Die phosphomonoesterase und die phosphodiesterase, The Journal of Biochemistry. 15 (1932) 19–28.

[15] L.B. Dolapchiev, R.A. Vassileva, K.S. Koumanov, Venom exonuclease. II. Amino acid composition and carbohydrate, metal ion and lipid content in the *Crotalus adamanteus* venom exonuclease, Biochim. Biophys. Acta. 622 (1980) 331–336. https://doi.org/10.1016/0005-2795(80)90044-6.

[16] R.M. Kini, T.V. Gowda, Rapid method for separation and purification of four isoenzymes of phosphodiesterase from *Trimeresurus flavoviridis* (habu snake) venom, Journal of Chromatography A. 291 (1984) 299–305. https://doi.org/10.1016/S0021-9673(00)95032-5.

[17] S.S.M. Al-Saleh, S. Khan, Purification and characterization of phosphodiesterase I from *Walterinnesia aegyptia* venom, Prep. Biochem. Biotechnol. 41 (2011) 262–77. https://doi.org/10.1080/10826068.2011.575319.

[18] S. Perron, S.P. Mackessy, R.M. Hyslop, Purification and characterization of exonuclease from rattlesnake venom, J. Colo.-Wyo. Acad. Sci. 25 (1993) 21–22.

[19] J.W. Fox, A brief review of the scientific history of several lesser-known snake venom proteins: l-amino acid oxidases, hyaluronidases and phosphodiesterases, Toxicon. 62 (2013) 75–82. https://doi.org/10.1016/j.toxicon.2012.09.009.

[20] N. Mori, T. Nikai, H. Sugihara, Phosphodiesterase from the venom of *Crotalus ruber ruber*, Int. J. Biochem. 19 (1987) 115–119. https://doi.org/10.1016/0020-711x(87)90321-1.

[21] A.A. Valério, A.C. Corradini, P.C. Panunto, S.M. Mello, S. Hyslop, Purification and characterization of a phosphodiesterase from *Bothrops alternatus* snake venom, J. Protein Chem. 21

(2002) 495–503. https://doi.org/10.1023/a:1022414503995.

[22] K. Trummal, A. Aaspõllu, K. Tõnismägi, M. Samel, J. Subbi, J. Siigur, E. Siigur, Phosphodiesterase from *Vipera lebetina* venom - structure and characterization, Biochimie. 106 (2014) 48–55. https://doi.org/10.1016/j.biochi.2014.07.020.

[23] M. Segovia, F.L. Figueroa, Detection of a 3′, 5′-cyclic-AMP phosphodiesterase activity in the lichenized fungus *Evernia prunastri*, Plant Biosystems - An International Journal Dealing with All Aspects of Plant Biology. 141 (2007) 123–127. https://doi.org/10.1080/11263500601153610.

[24] M.J. Perry, G.A. Higgs, Chemotherapeutic potential of phosphodiesterase inhibitors, Curr Opin Chem Biol. 2 (1998) 472–481. https://doi.org/10.1016/s1367-5931(98)80123-3.

[25] Y.H. Jeon, Y.-S. Heo, C.M. Kim, Y.-L. Hyun, T.G. Lee, S. Ro, J.M. Cho, Phosphodiesterase: overview of protein structures, potential therapeutic applications and recent progress in drug development, Cell. Mol. Life Sci. 62 (2005) 1198–1220. https://doi.org/10.1007/s00018-005-4533-5.

[26] L. Peng, X. Xu, D. Shen, Y. Zhang, J. Song, X. Yan, M. Guo, Purification and partial characterization of a novel phosphodiesterase from the venom of *Trimeresurus stejnegeri*: inhibition of platelet aggregation, Biochimie. 93 (2011) 1601–1609. https://doi.org/10.1016/j.biochi.2011.05.027.

[27] S. Pérez-Torres, R. Cortés, M. Tolnay, A. Probst, J.M. Palacios, G. Mengod, Alterations on phosphodiesterase type 7 and 8 isozyme mRNA expression in Alzheimer's disease brains examined by in situ hybridization, Exp. Neurol. 182 (2003) 322–334. https://doi.org/10.1016/s0014-4886(03)00042-6.

[28] A. Castro, M.J. Jerez, C. Gil, A. Martinez, Cyclic nucleotide phosphodiesterases and their role in immunomodulatory responses: advances in the development of specific phosphodiesterase inhibitors, Med Res Rev. 25 (2005) 229–244. https://doi.org/10.1002/med.20020.

[29] C.L. Miller, C. Yan, Targeting cyclic nucleotide phosphodiesterase in the heart: therapeutic implications, J Cardiovasc Transl Res. 3 (2010) 507–515. https://doi.org/10.1007/s12265-010-9203-9.

[30] S. Uckert, P. Hedlund, K.-E. Andersson, M.C. Truss, U. Jonas, C.G. Stief, Update on

phosphodiesterase (PDE) isoenzymes as pharmacologic targets in urology: present and future, Eur. Urol. 50 (2006) 1194–1207; discussion 1207. https://doi.org/10.1016/j.eururo.2006.05.025.

[31] C. Mehats, C.B. Andersen, M. Filopanti, S.-L.C. Jin, M. Conti, Cyclic nucleotide phosphodiesterases and their role in endocrine cell signaling, Trends in Endocrinology & Metabolism. 13 (2002) 29–35. https://doi.org/10.1016/S1043-2760(01)00523-9.

[32] M. Massimi, S. Cardarelli, F. Galli, M.F. Giardi, F. Ragusa, N. Panera, B. Cinque, M.G. Cifone, S. Biagioni, M. Giorgi, Increase of Intracellular Cyclic AMP by PDE4 Inhibitors Affects HepG2 Cell Cycle Progression and Survival, Journal of Cellular Biochemistry. 118 (2017) 1401–1411. https://doi.org/10.1002/jcb.25798.

[33] I.S. de Oliveira, I.A. Cardoso, K. de C.F. Bordon, S.E.A. Carone, J. Boldrini-França, M.B. Pucca, K.F. Zoccal, L.H. Faccioli, S.V. Sampaio, J.C. Rosa, E.C. Arantes, Global proteomic and functional analysis of *Crotalus durissus collilineatus* individual venom variation and its impact on envenoming, J Proteomics. 191 (2019) 153–165. https://doi.org/10.1016/j.jprot.2018.02.020.

[34] F.G. Amorim, R. Morandi-Filho, P.F. Fujimura, C. Ueira-Vieira, S.V. Sampaio, New findings from the first transcriptome of the *Bothrops moojeni* snake venom gland, Toxicon. 140 (2017) 105–117. https://doi.org/10.1016/j.toxicon.2017.10.025.

[35] E.L.H. Tang, C.H. Tan, S.Y. Fung, N.H. Tan, Venomics of *Calloselasma rhodostoma*, the Malayan pit viper: a complex toxin arsenal unraveled, J Proteomics. 148 (2016) 44–56. https://doi.org/10.1016/j.jprot.2016.07.006.

[36] Z.-M. Yang, Y.-E. Yang, Y. Chen, J. Cao, C. Zhang, L.-L. Liu, Z.-Z. Wang, X.-M. Wang, Y.-M. Wang, I.-H. Tsai, Transcriptome and proteome of the highly neurotoxic venom of *Gloydius intermedius*, Toxicon. 107 (2015) 175–186. https://doi.org/10.1016/j.toxicon.2015.08.010.

[37] F.G. Amorim, T.R. Costa, D. Baiwir, E. De Pauw, L. Quinton, S.V. Sampaio, Proteopeptidomic, functional and immunoreactivity characterization of *Bothrops moojeni* snake venom: influence of snake gender on venom composition, Toxins (Basel). 10 (2018).

https://doi.org/10.3390/toxins10050177.

[38] J. Boldrini-França, C.T. Cologna, M.B. Pucca, K. de C.F. Bordon, F.G. Amorim, F.A.P. Anjolette, F.A. Cordeiro, G.A. Wiezel, F.A. Cerni, E.L. Pinheiro-Junior, P.Y.T. Shibao, I.G. Ferreira, I.S. de Oliveira, I.A. Cardoso, E.C. Arantes, Minor snake venom proteins: Structure, function and potential applications, Biochim Biophys Acta Gen Subj. 1861 (2017) 824–838. https://doi.org/10.1016/j.bbagen.2016.12.022.

[39] F.E. Russell, F.W. Buess, M.Y. Woo, Zootoxicological properties of venom phosphodiesterase, Toxicon. 1 (1963) 99–108. https://doi.org/10.1016/0041-0101(63)90070-9.

[40] S.D. Aird, Ophidian envenomation strategies and the role of purines, Toxicon. 40 (2002) 335–393. https://doi.org/10.1016/s0041-0101(01)00232-x.

[41] M.L. Santoro, T.S. Vaquero, A.F. Paes Leme, S.M.T. Serrano, NPP-BJ, a nucleotide pyrophosphatase/phosphodiesterase from *Bothrops jararaca* snake venom, inhibits platelet aggregation, Toxicon. 54 (2009) 499–512. https://doi.org/10.1016/j.toxicon.2009.05.016.

[42] J. Mitra, D. Bhattacharyya, Phosphodiesterase from *Daboia russelli russelli* venom: purification, partial characterization and inhibition of platelet aggregation, Toxicon. 88 (2014) 1–10. https://doi.org/10.1016/j.toxicon.2014.06.004.

[43] W. Björk, Purification of phosphodiesterase from *Bothrops atrox* venom, with special consideration of the elimination of monophosphatases, J. Biol. Chem. 238 (1963) 2487–2490.

[44] U.K. Laemmli, Cleavage of structural proteins during the assembly of the head of bacteriophage T4, Nature. 227 (1970) 680–685. https://doi.org/10.1038/227680a0.

[45] P. Edman, G. Begg, A Protein Sequenator, Eur J Biochem. 1 (1967) 80–91. https://doi.org/10.1111/j.1432-1033.1967.tb00047.x.

[46] S.F. Altschul, T.L. Madden, A.A. Schäffer, J. Zhang, Z. Zhang, W. Miller, D.J. Lipman, Gapped BLAST and PSI-BLAST: a new generation of protein database search programs, Nucleic Acids Res. 25 (1997) 3389–3402. https://doi.org/10.1093/nar/25.17.3389.

[47] D. Morsa, D. Baiwir, R. La Rocca, T.A. Zimmerman, E. Hanozin, E. Grifnée, R. Longuespée, M.-A. Meuwis, N. Smargiasso, E.D. Pauw, G. Mazzucchelli, Multi-Enzymatic Limited Digestion: The Next-Generation Sequencing for Proteomics?, J. Proteome Res. 18 (2019) 2501–2513. https://doi.org/10.1021/acs.jproteome.9b00044.

[48] The UniProt Consortium, UniProt: a worldwide hub of protein knowledge, Nucleic Acids Research. 47 (2019) D506–D515. https://doi.org/10.1093/nar/gky1049.

[49] A. Marchler-Bauer, M.K. Derbyshire, N.R. Gonzales, S. Lu, F. Chitsaz, L.Y. Geer, R.C. Geer, J. He, M. Gwadz, D.I. Hurwitz, C.J. Lanczycki, F. Lu, G.H. Marchler, J.S. Song, N. Thanki, Z. Wang, R.A. Yamashita, D. Zhang, C. Zheng, S.H. Bryant, CDD: NCBI's conserved domain database, Nucleic Acids Research. 43 (2015) D222–D226. https://doi.org/10.1093/nar/gku1221.

[50] T. Schwede, J. Kopp, N. Guex, M.C. Peitsch, SWISS-MODEL: An automated protein homology-modeling server, Nucleic Acids Res. 31 (2003) 3381–3385. https://doi.org/10.1093/nar/gkg520.

[51] A. Waterhouse, M. Bertoni, S. Bienert, G. Studer, G. Tauriello, R. Gumienny, F.T. Heer, T.A.P. de Beer, C. Rempfer, L. Bordoli, R. Lepore, T. Schwede, SWISS-MODEL: homology modelling of protein structures and complexes, Nucleic Acids Res. 46 (2018) W296–W303. https://doi.org/10.1093/nar/gky427.

[52] A. Grosdidier, V. Zoete, O. Michielin, SwissDock, a protein-small molecule docking web service based on EADock DSS, Nucleic Acids Res. 39 (2011) W270-277. https://doi.org/10.1093/nar/gkr366.

[53] A. Grosdidier, V. Zoete, O. Michielin, Fast docking using the CHARMM force field with EADock DSS, J Comput Chem. 32 (2011) 2149–2159. https://doi.org/10.1002/jcc.21797.

[54] RomanA. Laskowski, J.AntoonC. Rullmann, MalcolmW. MacArthur, R. Kaptein, JanetM. Thornton, AQUA and PROCHECK-NMR: Programs for checking the quality of protein structures solved by NMR, J Biomol NMR. 8 (1996). https://doi.org/10.1007/BF00228148.

[55] R.A. Laskowski, M.W. MacArthur, D.S. Moss, J.M. Thornton, PROCHECK: a program to check the stereochemical quality of protein structures, J Appl Crystallogr. 26 (1993) 283–291. https://doi.org/10.1107/S0021889892009944.

[56] C. Colovos, T.O. Yeates, Verification of protein structures: Patterns of nonbonded atomic interactions, Protein Sci. 2 (1993) 1511–1519. https://doi.org/10.1002/pro.5560020916.

[57] E.F. Pettersen, T.D. Goddard, C.C. Huang, G.S. Couch, D.M. Greenblatt, E.C. Meng, T.E. Ferrin, UCSF Chimera--a visualization system for exploratory research and analysis, J Comput Chem. 25 (2004) 1605–1612. https://doi.org/10.1002/jcc.20084.

[58] F.H. Niesen, H. Berglund, M. Vedadi, The use of differential scanning fluorimetry to detect ligand interactions that promote protein stability, Nature Protocols. 2 (2007) 2212–2221. https://doi.org/10.1038/nprot.2007.321.

[59] S. Saha, G.P.S. Raghava, Prediction of continuous B-cell epitopes in an antigen using recurrent neural network, Proteins. 65 (2006) 40–48. https://doi.org/10.1002/prot.21078.

[60] J.M. Medeiros, I.S. Oliveira, I.G. Ferreira, G.M. Alexandre-Silva, F.A. Cerni, U. Zottich, M. B. Pucca, Fatal Rattlesnake Envenomation in Northernmost Brazilian Amazon: A Case Report and Literature Overview, Reports. 3 (2020) 9. https://doi.org/10.3390/reports3020009.

[61] M.H. da Silva, O.G. Bier, Titration of antiserum to South American rattlesnake (*Crotalus durissus terrificus*) venom by inhibition of phospholipase A2 activity, Toxicon. 20 (1982) 563–569. https://doi.org/10.1016/0041-0101(82)90050-2.

[62] G.R. Philipps, Purification and characterization of phosphodiesterase from Crotalus venom, Hoppe-Seyler's Z. Physiol. Chem. 356 (1975) 1085–1096. https://doi.org/10.1515/bchm2.1975.356.2.1085.

[63] H. Sugihara, T. Nikai, M. Naruse, M. Kishida, N. Mori, Purification and characterization of phosphodiesterase from the venom of *Trimeresurus mucrosquamatus*, Int. J. Biochem. 18 (1986) 203–207. https://doi.org/10.1016/0020-711x(86)90106-0.

[64] S.S.M. Al-Saleh, S.U. Khan, M. Ashraf, Biochemical characterization and some biological properties of the phosphodiesterase I purified from *Agistrodon bilineatus* venom, Indian J Biochem Biophys. 46 (2009) 221–229.

[65] A. Ullah, K. Ullah, H. Ali, C. Betzel, S. ur Rehman, The Sequence and a Three-Dimensional Structural Analysis Reveal Substrate Specificity among Snake Venom Phosphodiesterases, Toxins. 11 (2019) 625. https://doi.org/10.3390/toxins11110625.

[66] H.Y. Halim, E.A. Shaban, M.M. Hagag, E.W. Daoud, M.F. el-Asmar, Purification and characterization of phosphodiesterase (exonuclease) from *Cerastes cerastes* (Egyptian sand viper) venom, Toxicon. 25 (1987) 1199–1207. https://doi.org/10.1016/0041-0101(87)90138-3.

[67] K.W. Moremen, M. Tiemeyer, A.V. Nairn, Vertebrate protein glycosylation: diversity, synthesis and function, Nat. Rev. Mol. Cell Biol. 13 (2012) 448–462. https://doi.org/10.1038/nrm3383.

[68] S.R. Stowell, T. Ju, R.D. Cummings, Protein glycosylation in cancer, Annu Rev Pathol. 10 (2015) 473–510. https://doi.org/10.1146/annurev-pathol-012414-040438.

[69] R. Doley, R.M. Kini, Protein complexes in snake venom, Cell. Mol. Life Sci. 66 (2009) 2851–2871. https://doi.org/10.1007/s00018-009-0050-2.

[70] N.R. Casewell, S.C. Wagstaff, W. Wüster, D.A.N. Cook, F.M.S. Bolton, S.I. King, D. Pla, L. Sanz, J.J. Calvete, R.A. Harrison, Medically important differences in snake venom composition are dictated by distinct postgenomic mechanisms, Proc. Natl. Acad. Sci. U.S.A. 111 (2014) 9205–9210. https://doi.org/10.1073/pnas.1405484111.

[71] D. Andrade-Silva, A. Zelanis, E.S. Kitano, I.L.M. Junqueira-de-Azevedo, M.S. Reis, A.S. Lopes, S.M.T. Serrano, Proteomic and Glycoproteomic Profilings Reveal That Post-translational Modifications of Toxins Contribute to Venom Phenotype in Snakes, J. Proteome Res. 15 (2016) 2658–2675. https://doi.org/10.1021/acs.jproteome.6b00217.

[72] G. Zancolli, L. Sanz, J.J. Calvete, W. Wüster, Venom On-a-Chip: A Fast and Efficient Method for Comparative Venomics, Toxins (Basel). 9 (2017). https://doi.org/10.3390/toxins9060179.

[73] Z. Levy, A. Bdolah, Multiple molecular forms of snake venom phosphodiesterase from *Vipera palastinae*, Toxicon. 14 (1976) 389–390. https://doi.org/10.1016/0041-0101(76)90086-6.

[74] G.R. Philipps, Purification and characterization of phosphodiesterase I from *Bothrops atrox*, Biochim. Biophys. Acta. 432 (1976) 237–244. https://doi.org/10.1016/0005-2787(76)90165-9.

[75] N.M. Ibrahim, W.H. Salama, A.E.E. Hakim, Phosphodiesitrase activity of some Egyptian snake venoms: biochemical and immunological characteristics and effect on blood coagulation of phosphodiesterase enzyme from *Naja nigricollis* venom, J Chem Pharm Res. 8 (2016) 11.

[76] J.G. Zalatan, T.D. Fenn, A.T. Brunger, D. Herschlag, Structural and Functional Comparisons of Nucleotide Pyrophosphatase/Phosphodiesterase and Alkaline Phosphatase: Implications for Mechanism and Evolution, Biochemistry. 45 (2006) 9788–9803. https://doi.org/10.1021/bi060847t.

[77] WHO, Snakebite envenoming - Key facts 2019, (2019). https://www.who.int/news-room/fact-sheets/detail/snakebite-envenoming (accessed April 22, 2020).

[78] A.H. Laustsen, J. María Gutiérrez, C. Knudsen, K.H. Johansen, E. Bermúdez-Méndez, F.A. Cerni, J.A. Jürgensen, L. Ledsgaard, A. Martos-Esteban, M. Øhlenschlæger, U. Pus, M.R. Andersen, B. Lomonte, M. Engmark, M.B. Pucca, Pros and cons of different therapeutic antibody formats for recombinant antivenom development, Toxicon. 146 (2018) 151–175. https://doi.org/10.1016/j.toxicon.2018.03.004.

[79] R.D. Bremel, E.J. Homan, An integrated approach to epitope analysis I: Dimensional reduction, visualization and prediction of MHC binding using amino acid principal components and regression approaches, Immunome Res. 6 (2010) 7. https://doi.org/10.1186/1745-7580-6-7.

[80] G.N. Sivalingam, A.J. Shepherd, An analysis of B-cell epitope discontinuity, Molecular Immunology. 51 (2012) 304–309. https://doi.org/10.1016/j.molimm.2012.03.030.

[81] E. Oyama, N. Furudate, K. Senuki, H. Takahashi, Purification and characterization of a new platelet aggregation inhibitor with dissociative effect on ADP-induced platelet aggregation, from the venom of Protobothrops elegans (Sakishima-habu), Toxicon. 53 (2009) 706–712.

https://doi.org/10.1016/j.toxicon.2009.02.016.

[82] S.P. Kunapuli, R.T. Dorsam, S. Kim, T.M. Quinton, Platelet purinergic receptors, Current Opinion in Pharmacology. 3 (2003) 175–180. https://doi.org/10.1016/S1471-4892(03)00007-9.

[83] G.F. King, Venoms as a platform for human drugs: translating toxins into therapeutics, Expert Opinion on Biological Therapy. 11 (2011) 1469–1484. https://doi.org/10.1517/14712598.2011.621940.

[84] K. de C.F. Bordon, C.T. Cologna, E.C. Fornari-Baldo, E.L. Pinheiro-Júnior, F.A. Cerni, F.G. Amorim, F.A.P. Anjolette, F.A. Cordeiro, G.A. Wiezel, I.A. Cardoso, I.G. Ferreira, I.S. de Oliveira, J. Boldrini-França, M.B. Pucca, M.A. Baldo, E.C. Arantes, From Animal Poisons and Venoms to Medicines: Achievements, Challenges and Perspectives in Drug Discovery, Front. Pharmacol. 11 (2020) 1132. https://doi.org/10.3389/fphar.2020.01132.

[85] S.E. Gasanov, M.A. Alsarraj, N.E. Gasanov, E.D. Rael, Cobra Venom Cytotoxin Free of Phospholipase A 2 and Its Effect on Model Membranes and T Leukemia Cells, Journal of Membrane Biology. 155 (1997) 133–142. https://doi.org/10.1007/s002329900165.

[86] I.S. de Oliveira, R.V. Manzini, I.G. Ferreira, I.A. Cardoso, K. de C.F. Bordon, A.R.T. Machado, L.M.G. Antunes, J.C. Rosa, E.C. Arantes, Cell migration inhibition activity of a non-RGD disintegrin from Crotalus durissus collilineatus venom, J Venom Anim Toxins Incl Trop Dis. 24 (2018) 28. https://doi.org/10.1186/s40409-018-0167-6.

[87] D.A. Maria, R.C. Vassão, I.R.G. Ruiz, Haematopoietic effects induced in mice by the snake venom toxin jararhagin, Toxicon. 42 (2003) 579–585. https://doi.org/10.1016/S0041-0101(03)00237-X.

[88] M.B. Pucca, S. Peigneur, C.T. Cologna, F.A. Cerni, K.F. Zoccal, K. de C.F. Bordon, L.H. Faccioli, J. Tytgat, E.C. Arantes, Electrophysiological characterization of the first *Tityus serrulatus* alpha-like toxin, Ts5: Evidence of a pro-inflammatory toxin on macrophages, Biochimie. 115 (2015) 8–16. https://doi.org/10.1016/j.biochi.2015.04.010.

[89] M.B. Pucca, S. Ahmadi, F.A. Cerni, L. Ledsgaard, C.V. Sørensen, F.T.S. McGeoghan, T.

Stewart, E. Schoof, B. Lomonte, U. auf dem Keller, E.C. Arantes, F. Çalışkan, A.H. Laustsen, Unity Makes Strength: Exploring Intraspecies and Interspecies Toxin Synergism between Phospholipases A2 and Cytotoxins, Front. Pharmacol. 11 (2020) 611. https://doi.org/10.3389/fphar.2020.00611.

[90] S. Ahmadi, M.B. Pucca, J.A. Jürgensen, R. Janke, L. Ledsgaard, E.M. Schoof, C.V. Sørensen, F. Çalışkan, A.H. Laustsen, An in vitro methodology for discovering broadly-neutralizing monoclonal antibodies, Sci Rep. 10 (2020) 10765. https://doi.org/10.1038/s41598-020-67654-7.

[91] M. Rivel, D. Solano, M. Herrera, M. Vargas, M. Villalta, Á. Segura, A.S. Arias, G. León, J.M. Gutiérrez, Pathogenesis of dermonecrosis induced by venom of the spitting cobra, *Naja nigricollis*: An experimental study in mice, Toxicon. 119 (2016) 171–179. https://doi.org/10.1016/j.toxicon.2016.06.006.

[92] G.D. Laing, P.B. Clissa, R.D.G. Theakston, A.M. Moura-da-Silva, M.J. Taylor, Inflammatory pathogenesis of snake venom metalloproteinase-induced skin necrosis, Eur. J. Immunol. 33 (2003) 3458–3463. https://doi.org/10.1002/eji.200324475.

[93] C.M. Sant'Ana Malaque, J.M. Gutiérrez, Snakebite Envenomation in Central and South America, in: J. Brent, K. Burkhart, P. Dargan, B. Hatten, B. Megarbane, R. Palmer (Eds.), Critical Care Toxicology, Springer International Publishing, Cham, 2015: pp. 1–22. https://doi.org/10.1007/978-3-319-20790-2_146-1.

Table 1. Protein recovery from *Cdc*PDE during the purification steps.

Sample	Purification Step	Protein recovery (%)*	Total protein (mg)	Total activity (U)	Specific activity (U/mg)	Purification fator	Yield (%)
Snake venom	Supernatant	100.00	90.00	125.10	1.39	1	100

S3	Gel filtration	2.87	2.58	68.89	27.09	19.49	55
A1	Anion Exchange	0.83	0.75	106.49	141.99	102.15	85
C2	Cation Exchange	0.71	0.64	68.80	107.50	77.34	55

*Recovery percentage calculated using Unicorn 5.2 software (GE Healthcare) according to the ratio between the area under the absorbance curve at 280 nm of each corresponding fraction and the sum of the areas of all fractions eluted. One unit of enzymatic activity (U) corresponds to an increase of 1.0 $Abs_{400\ nm}$/min.

Figure 1. Chromatographic and enzymatic activity profiles of the venom and fractions using an FPLC system. (A) *Cdc* venom (90 mg) was filtered on a HiPrep Sephacryl S-200 HR column (16 × 600 mm, 47 µm particles), using isocratic gradient of 50 mM Tris-HCl containing 150 mM NaCl, pH 8, at a flow rate of 0.5 mL/min. Inset panel – whole chromatographic profile without magnification. **(B)** Anion exchange chromatography of fraction S3 (6 mg) on a HiTrap ANX (high sub) FF column (16 × 25 mm), using a linear gradient (0-100%) of buffer B (50 mM Tris-HCl with 1 M NaCl, pH 8, dashed blue line), at a flow rate of 3 mL/min. Buffer A is 50 mM Tris-HCl, pH 8. **(C)** Cation ion-exchange chromatography of fraction A1 (0.7 mg) on a carboxymethyl cellulose-52 column (10 × 100 mm), using a segmented concentration gradient (0-100%) of buffer B (50 mM sodium acetate with 1 M NaCl, pH 5, dashed blue line), at a flow rate of 0.5 mL/min. Buffer A is 50 mM sodium acetate, pH 5. **(D)** Reversed-phase chromatography of fraction C2 (1 mg) on a C4 Jupiter column (4.6 × 250 mm, 300 Å, 5 µm particles), using a linear gradient (0-100%) of solution B (80% acetonitrile, in 0.1% TFA,

dashed blue line), at a flow rate of 1 mL/min. Solution A is 0.1% TFA. Pink vertical lines represent relative *Cdc*PDE activity of fractions (50 µL) using *bis*(*p*-nitrophenyl) phosphate substrate.

Figure 2. Electrophoretic profile and mass determination of *Cdc*PDE at different conditions. SDS-PAGE (10%) under **(A)** non-reducing and **(B)** reducing conditions. **(C)** Evaluation of *Cdc*PDE N-glycosylation. M1: Molecular mass marker (97.0-14.4 kDa); M2: Wide range molecular mass marker (120-10 kDa); SV: *C. d. collilineatus* venom; S3, A1 and C2: Fractions obtained, respectively, in the first, second, and third chromatographic step; R: Fraction obtained through reversed-phase chromatography; Black arrow indicates PNGase enzyme; PDE_d: reduced and deglycosylated *Cdc*PDE; PDE_r: reduced *Cdc*PDE. **(D)** Mass spectrum of *Cdc*PDE obtained by MALDI-TOF (positive linear mode) using sinapinic acid (SA) matrix.

Figure 3. PDE activity assays. The substrate *bis*(*p*-nitrophenyl) phosphate (1 mM) was added to a mixture (150 µL) of *Cdc*PDE (0.175 µg) and 100 mM Tris-HCl, pH 8, previously incubated for 10 min at 37 ºC. This new mixture was incubated for 30 mins at 37 ºC. The reaction was stopped with 50 mM sodium hydroxide (NaOH). Absorbance was measured at 400 nm. The enzymatic activity was expressed as a percentage of relative activity to that of highest absorbance. The values represent the mean ± standard deviation (SD, n = 3). **(A)** pH profile. The enzymatic activity assay was performed by incubating *Cdc*PDE and substrate in 100 mM Tris-HCl buffers at different pHs for 30 min, at 37 ºC. **(B)** Storage temperature profile. The enzymatic activity assay was performed with *Cdc*PDE previously stored at different temperatures for 1 hour. **(C)** Temperature profile. The enzymatic activity assay was performed by incubating *Cdc*PDE and substrate in 100 mM Tris-HCl (pH 8) at different temperatures for 30 min. **(D)** Michaelis-Menten fitting for *Cdc*PDE (5 µg, 0.537 U, 5 µM) kinetics curve, using the substrate *bis*(*p*-nitrophenyl) phosphate. **(E)** *Cdc*PDE and different inhibitors (0.625-10 mM) were previously incubated for 30 min at 37 ºC. As a positive control (without inhibitor), PDE was previously incubated only with buffer (100 mM Tris-HCl, pH 8).

Figure 4. PDE thermal stability. *Cdc*PDE (2 µg) was incubated with water and different 50 mM buffering conditions (sodium acetate, pH 4.5; sodium citrate, pH 5; succinate, pH 5.5; MES, pH 6; bis-Tris, pH 6.5; imidazole, pH 7; 4-(2-hydroxyethyl)-1-piperazineethanesulfonic acid (HEPES), pH 7.5; Tris-HCl, pH 8; bis-Tris propane, pH 8.5; 2-amino-2-methyl-1,3-propanediol (AMPD), pH 9; and glycine, pH 9.5), containing different NaCl concentrations (0-1000 mM). The fluorescent Sypro Orange (50×) was added to the samples. Thermal denaturation was evaluated at a temperature ranging from 25 ºC to 95 ºC, with gradual increases of 1 ºC/min, followed by fluorescence reading using the excitation/emission wavelength of 492/610 nm in the real time thermocycler Mx3005P.

Figure 5. Sequence alignment of *Cdc*PDE and others snake venom PDEs. *Cdc*PDE, *C. adamanteus* (J3SEZ3 and J3SBP3), *Protobothrops flavoviridis* (T2HF62), and *Macrovipera lebetina* (W8E7D1). Instead of the conserved residues, the following features are highlighted due to high identity: Low consensus amino acid residues (pink), signal peptide (gray), Cys residues (yellow), Asn-aaX-Ser/Thr residues, which represent the potential N-glycosylation sites (blue); and Asn-aaX-Ser/Thr residues, which represent N-glycosylation sites determined by MS/MS (green). Based on other snake venom PDE sequences, residue Thr (163), colored in red, potentially participates in catalytic activity.

Figure 6. Molecular modeling of *Cdc*PDE and docking simulation. (A) Front and **(B)** back view of *Cdc*PDE; 3D-structure of the molecule was estimated by Swiss-Model using the PDE from Taiwan cobra (*Naja atra*; PDB: 5GZ4) as a template. Disulfide bonds are shown in yellow, α-helices in red, β-sheets in blue, and N-terminal amino acid residues in the pink segment. The residue (T163) that may participate in *Cdc*PDE activity is highlighted. **(C)** Docking simulation with *bis*(*p*-nitrophenyl) phosphate substrate (blue, orange, and red molecule; PubChem CID: 255). **(D)** Magnified view and **(E)** substrate-enzyme interaction.

Figure 7. *Cdc*PDE recognition by anticrotalid antivenom in ELISA and prediction of the recognized epitopes. (A) *Cdc*PDE and *C. d. collilineatus* venom (2 µg each) were incubated with commercial anti-crotalid antivenom from Instituto Butantan. Absorbance was measured at 490 nm.

Data are presented as mean ± SD analyzed by one-way ANOVA and Tukey's multiple comparison test (quadruplicate assay). C(+): wells coated with non-immunized horse serum diluted 1:50; SV: *C. d. collilineatus* venom incubated with commercial anti-crotalid antivenom diluted 1:100; C(-) SV: *C. d. collilineatus* venom incubated with non-immunized horse serum diluted 1:100; PDE: *Cdc*PDE incubated with commercial anti-crotalid antivenom diluted 1:100; C(-) PDE: *Cdc*PDE incubated with non-immunized horse serum diluted 1:100. ****p< 0.0001 when compared to its negative control; $^{###}p$< 0.001 when compared to positive control; $^{####}p$< 0.0001 when compared to positive control. **(B)** *Cdc*PDE sequence with the epitopes predicted by ABCpred Server tool highlighted in blue.

Figure 8. Functional assays with *Cdc*PDE. (A) Inhibition of ADP-induced platelet aggregation by *Cdc*PDE. Different concentrations of *Cdc*PDE (15-120 µg/mL, 50 µL) were incubated with PRP (450 µL) at 37 ºC for 5 min under shaking. Then, ADP (2.4 µM) was added to the mixture and the aggregation was monitored for 6 min. C(-): water. ****p < 0.0001 when compared to negative control. **(B)** Effect of *Cdc*PDE on N/TERT cell viability. N/TERT cells were incubated with different concentrations of *Cdc*PDE (10-200 µg/mL) in DMEM medium. After 24 h, cell viability was measured by using CellTiter-Glo luminescent cell viability assay. ****p < 0.0001 when compared with negative control (cells incubated with saline solution) and the presented values are the mean ± SD (n = 3).

Figure 1

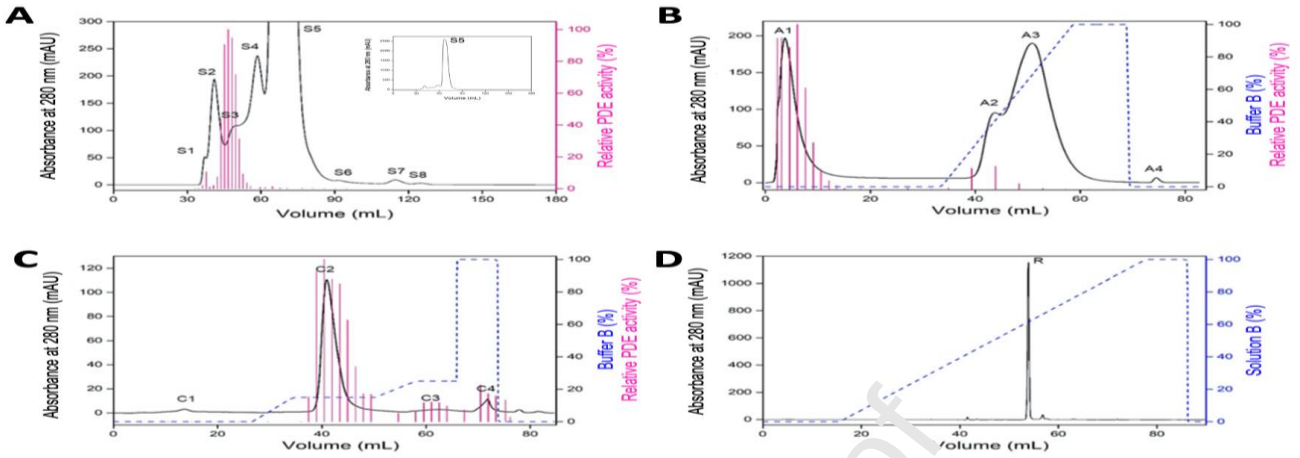

Figure 2

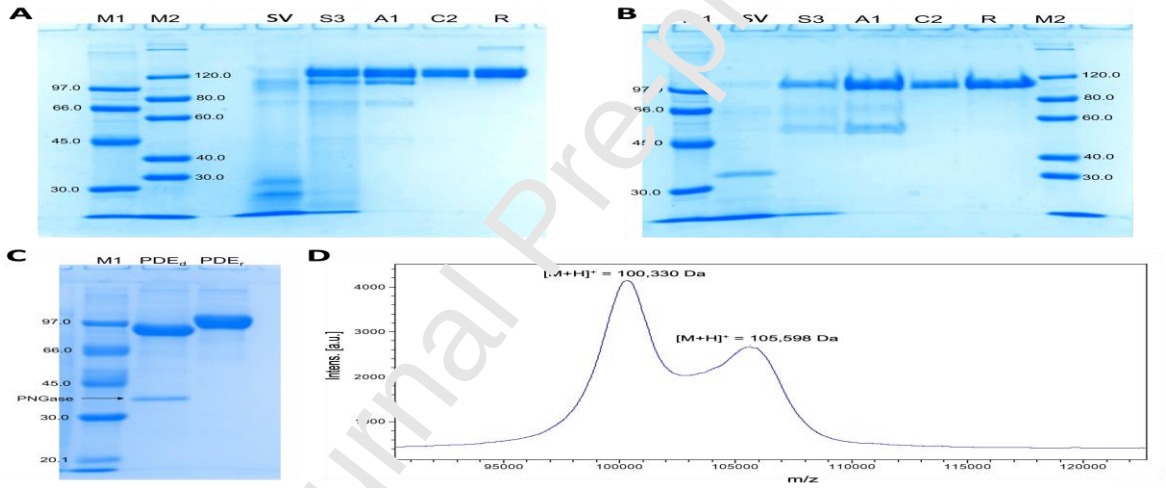

Figure 3

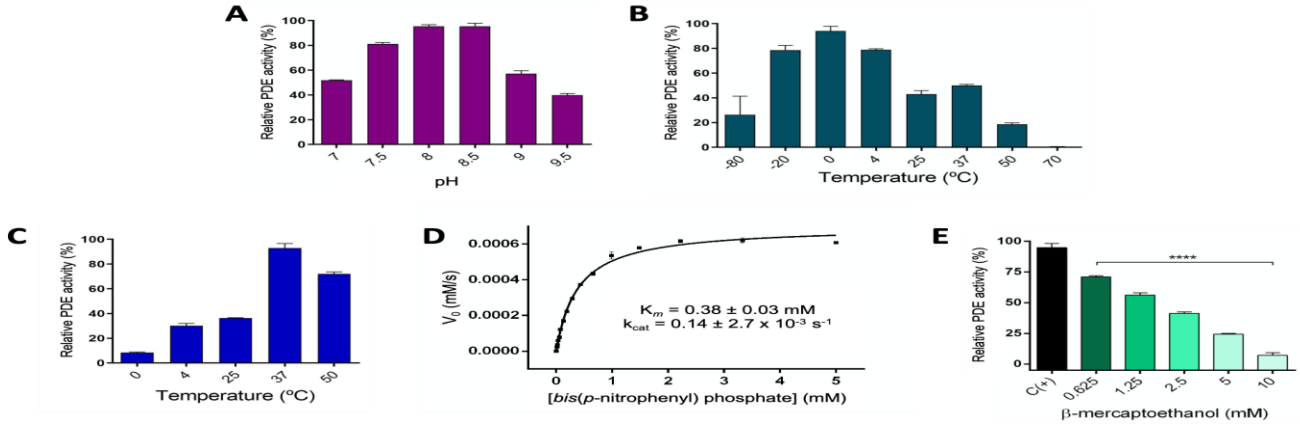

Figure 4

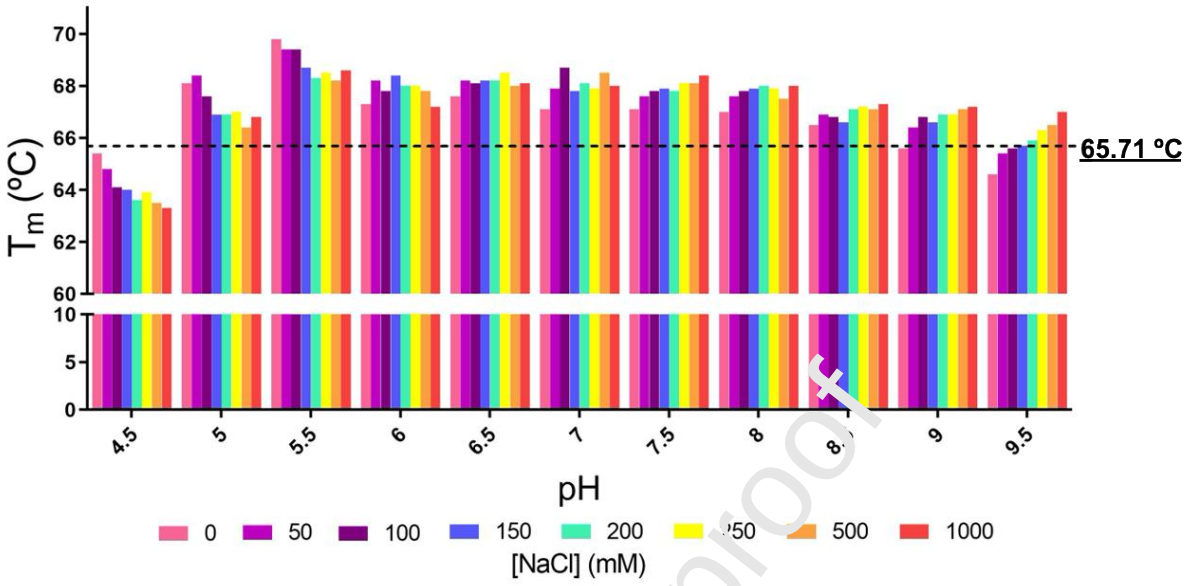

Figure 5

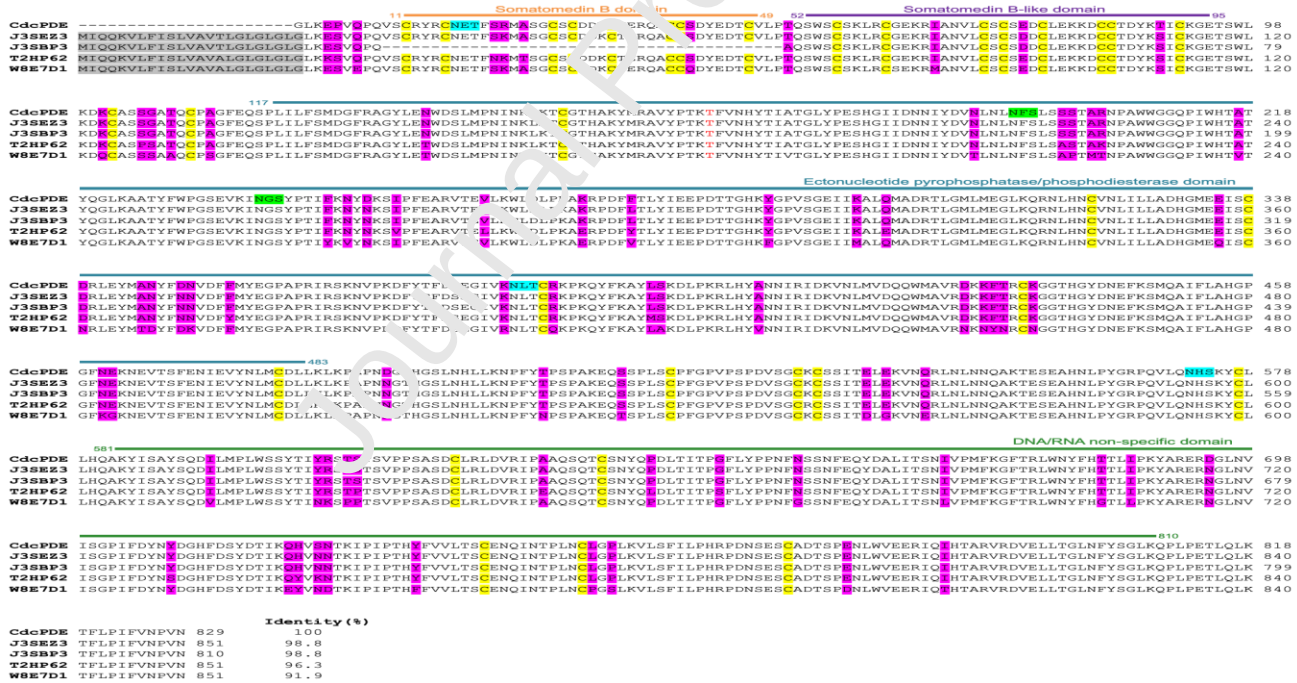

Figure 6

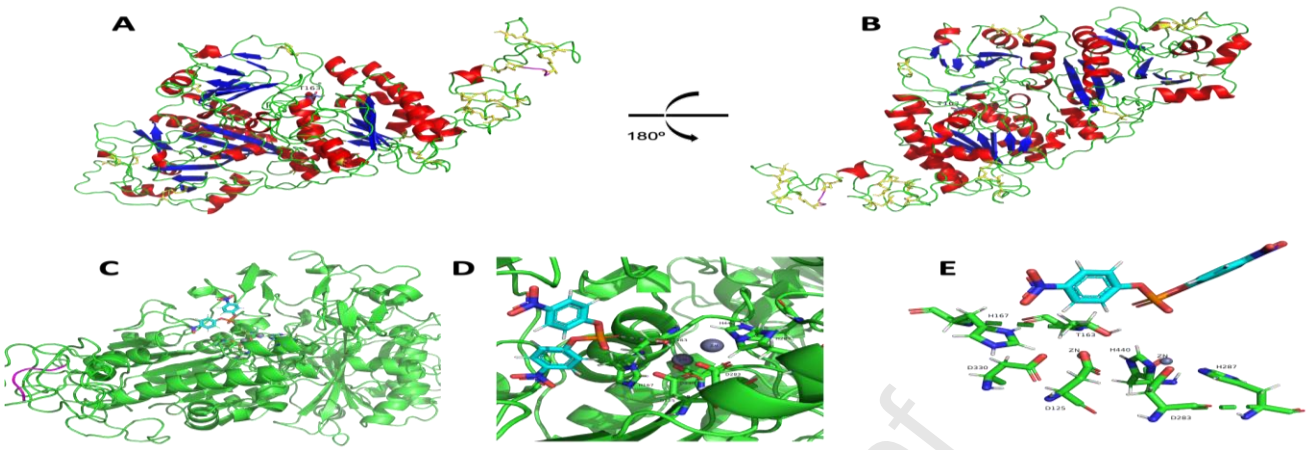

Figure 7

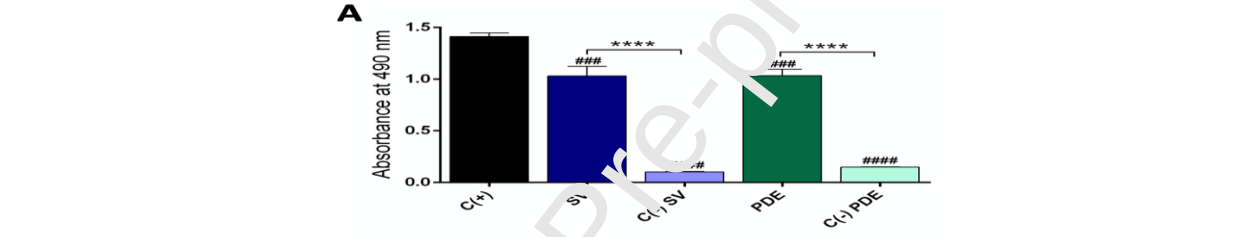

Figure 8

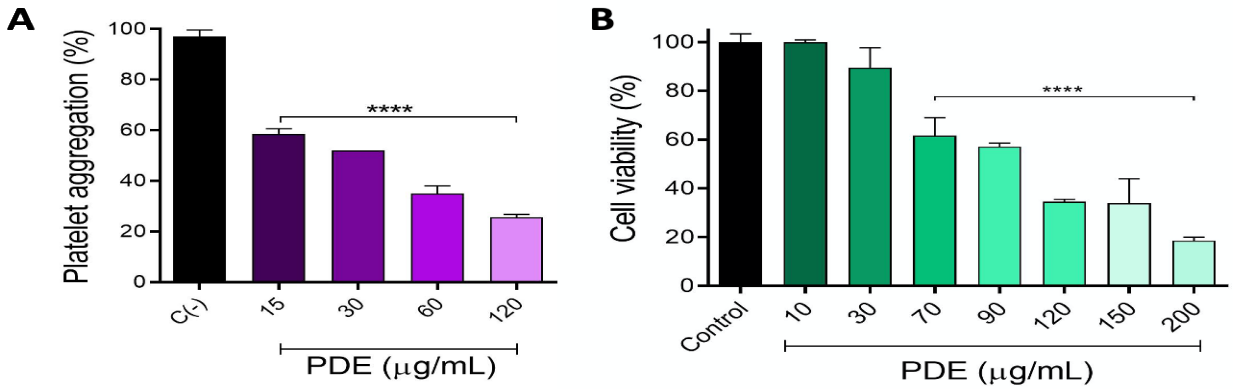

Highlights

- *Cdc*PDE is the first phosphodiesterase isolated from *C. d. collilineatus* snake venom;
- Metal ions and disulfide bonds are essential for its enzymatic activity;
- Crotalid antivenom is able to recognize *Cdc*PDE;
- *Cdc*PDE inhibits platelet ADP-induced aggregation;
- *Cdc*PDE is cytotoxic to human keratinocytes.